J|A|C|S COMMUNICATIONS

Published on Web 03/16/2009

Wet Chemistry Route to Hydrophobic Blue Fluorescent Nanodiamond

Vadym N. Mochalin and Yury Gogotsi*

Department of Materials Science and Engineering, Drexel University, 3141 Chestnut Street, Philadelphia, Pennsylvania 19104

Received January 26, 2009; E-mail: Gogotsi@drexel.edu

Recent years have been marked with a growing interest in the use of carbon nanomaterials in biomedical imaging. The idea stems from the unique properties of semiconductor quantum dots which demonstrate bright, stable, size-dependent fluorescence due to the quantum confinement effect.[1] However, their *in vivo* applications are limited by intrinsic toxicity due to the heavy metals and halcogenides they contain.

Semiconductor single-walled carbon nanotubes (SWCNTs) are fluorescent in NIR and, despite a low fluorescence quantum yield,[2] are traceable in living cells. Potential cytotoxicity, though debatable,[2] is still suspected for carbon nanotubes, which restrains their *in vivo* applications. Photoluminescent carbon dots were produced by laser ablation of graphite followed by oxidation with HNO_3 and functionalization with diamine-terminated polyethylene glycol.[3] Amorphous sp^2 carbon particles, derived from candle soot, show multicolor fluorescence.[4] Luminescent carbon nanoparticles were synthesized through thermal oxidation of sodium 11-amino-undecanoate citrate at 300 °C in air (oxygen-containing functionalized carbon dots)[5] and electrooxidation of graphite.[6] Fluorescent carbon spheres (~400 nm in diameter) produced by hydrothermal treatment of glucose have been used for intranuclear drug delivery in cells.[7]

Among other carbon allotropes, nanodiamond (ND) powders, produced by detonation synthesis have attracted much attention for biomedical applications because they show low or no cytotoxicity.[8,9] Therefore, ND is currently considered the most versatile platform for biomedical applications of nanoparticles, in particular, for *in vivo* imaging. Bright fluorescent 100 nm particles were produced by irradiation of synthetic type Ib diamond with a high-energy proton beam and subsequent annealing to form fluorescent $(N-V)^-$ centers with ~560 nm excitation and ~700 nm (red) emission.[9] The red fluorescence of the irradiated material is so intense that it allows for detection of a single 35 nm diamond nanoparticle in a cell.[10] The H3 defect center (N−V−N) in type Ia diamond has green fluorescence (531 nm emission wavelength). These fluorescent diamond nanoparticles produced by ion beam radiation are a promising alternative to semiconductor quantum dots because they are stable against photobleaching and can be linked to large biomolecules. Yet, the cost of their production is prohibitive for widespread use, and their size may be too large for penetration through cell membranes or overcoming the blood−brain barrier. No blue fluorescent ND has been reported so far.

In this study we report on the synthesis of hydrophobic blue fluorescent material (ND-ODA) by covalent linking of octadecylamine (ODA) to 5 nm ND particles. As the nanodiamond powders are produced by detonation on a large commercial scale, and the wet chemistry surface modification procedure is fairly simple, the resulting fluorescent nanodiamond can be used for a variety of applications. The technique to functionalize the ND with ODA via the amide bond formation (eq 1) is similar to that used for SWCNTs.[11]

The same surface modification can be used for other carbon nanoparticles. 30 mg of ND (UD90 grade, NanoBlox, Inc., USA), purified by air oxidation[12] and cleansed of metal impurities by boiling in 35 wt % HCl for 24 h (**1** in eq 1), was refluxed with 50 mL of $SOCl_2$ (Sigma Aldrich) and 1 mL of anhydrous *N*,*N*-dimethylformamide (DMF) (Sigma Aldrich), which is well known as a catalyst for this reaction, at 70 °C for 24 h.

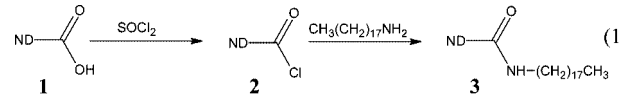

After removing the brown-colored liquid, solid **2** was washed with anhydrous tetrahydrofuran 2 times and then dried at ambient temperature in a desiccator under vacuum. ~30 mg of the acyl chloride derivative **2** was stirred in a sealed flask with 1 g of ODA (Sigma Aldrich) at 90−100 °C for 96 h. After cooling, excess ODA was removed by sonication with anhydrous methanol (Sigma Aldrich) 4−5 times. To remove adsorbed ODA, the material was further purified by extraction with hot methanol in a Soxhlet apparatus. To ensure complete extraction, it was repeated 10 times with fresh methanol. Purified ND-ODA powder **3** was used in subsequent studies. The sequence of reactions was monitored by FTIR analysis of the products **1**−**3** (Figure 1). C═O stretch vibrations in an acyl chloride derivative of ND (Figure 1, spectrum

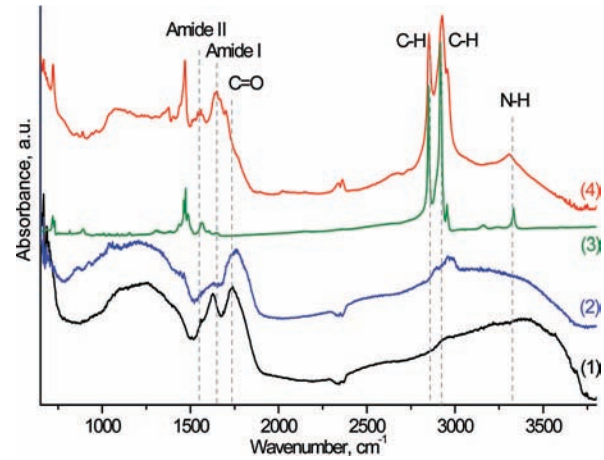

Figure 1. FTIR spectra of ND (1), ND acyl chloride (2), ODA (3), and ND-ODA (4).

2) are shifted to a higher frequency compared to the C═O band in ND, thus indicating the conversion of −COOH into −COCl (**1** to **2** in eq 1). Treatment of acyl chloride derivative **2** with ODA results in formation of the amide **3**. IR Amide I and Amide II bands at 1650 and 1550 cm^{-1}, respectively, in the spectrum of **3** (Figure 1, spectrum 4), provide a proof of covalent attachment of ODA through the amide bond formation, as opposed to physisorption of ODA. Other IR features of ND-ODA, such as strong C−H stretch vibrations at 2800−3000 cm^{-1} characteristic of long hydrocarbon

10.1021/ja9004514 CCC: $40.75

chains, and the N−H stretch of the amino group at 3300 cm^{-1}, cannot be considered alone as proof of the amide **3** formation, because they might appear in the spectrum simply as a result of ODA physisorption.

A UV Raman spectrum of ND-ODA (Supporting Information, Figure S1) shows typical features of nanodiamond: a broad and downshifted peak of diamond at 1327 cm^{-1} and a broad intense peak at 1630 cm^{-1}.[13] The unresolved peaks of C−H (at ∼2980 cm^{-1}) and N−H (at ∼3200 cm^{-1}) are also present in agreement with the structure **3**. These latter Raman peaks overlap with the second-order spectrum of sp^2 carbon in ND.

Due to the long hydrocarbon chains linked to its surface, the ND-ODA can be easily dispersed in hydrophobic solvents such as benzene, toluene, chloroform, dichloromethane, etc. (Figure 2). At

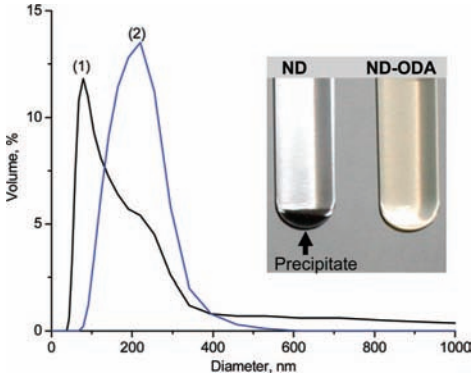

Figure 2. Particle size of ND-ODA in toluene (1) and chloroform (2); photograph of 0.01% wt suspensions of ND and ND-ODA in toluene.

the same time, it is immiscible with water and poorly miscible with hydrophilic organic solvents such as DMF, ethanol, methanol, and acetone. While ND, being dispersed in toluene with ultrasonication, completely precipitates within 1 h (Figure 2), ND-ODA without any sonication or other means forms a clear, stable pale yellowish (or brown at high concentrations) colloidal solution, which showed no visible precipitation during a week. The solubility of ND-ODA estimated gravimetrically is ∼4 g/L in dichloromethane and ∼3 g/L in toluene. Particle size measurements showed 100−300 nm ND-ODA agglomerates in toluene and chloroform (Figure 2 curves 1 and 2) in contrast to 5−9 μm agglomerates formed in DMF (not shown). Good solubility is extremely important for many applications of ND, and ND-ODA can be used in lubricant or motor oil additives as well as in other applications where stable nanodiamond suspensions in hydrophobic systems (fuels, polymers, or oils) are required. No sonication, surfactants, or other special means of dispersing are necessary for ND-ODA.

Another interesting property of ND-ODA is its bright blue fluorescence under UV light excitation, which easily can be seen even in a very diluted colloidal solution (Figure 3). The excitation maximum of ND-ODA is at 410 nm with emission at 450 nm (blue). Neither ND nor pure ODA shows any blue fluorescence, which is a result of ND functionalization with ODA. ND-ODA retained fluorescence after drying and 2 years of storage. Thus the fluorescence does not result from an interaction with solvent and is not specific for solvated ND.

The blue fluorescent ND-ODA adds another color to the set of red and green fluorescent NDs.[9,10] The mechanism of ND-ODA fluorescence needs further study. This phenomenon can be due to partial thermal degradation of the ODA chains linked to ND with (poly)aromatic structures formation. Better understanding the mechanism and applications of ND-ODA in biomedical imaging will be a subject of future studies.

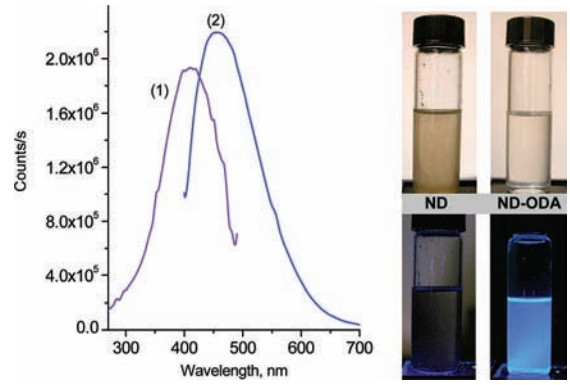

Figure 3. Excitation monitored at 450 nm emission (1) and emission at 410 nm excitation (2) spectra of ND-ODA dispersion in dichloromethane; photographs of ND and ND-ODA (0.004% wt) dispersions in dichloromethane with visible (upper row) and UV (365 nm, lower row) illumination.

Acknowledgment. We thank NanoBlox, Inc., USA and Ben Franklin Technology Partners of Southeastern Pennsylvania for financial support. We are grateful to Mr. Christopher Hobson (Drexel) for experimental help; Mr. Charles Picardi (NanoBlox) for helpful discussions; Dr. Z. Nikolov and the Centralized Research Facility (CRF) of the College of Engineering and Department of Chemistry for providing access to spectrometers.

Supporting Information Available: Complete ref 3, UV Raman spectrum of ND-ODA; FTIR, particle size distribution, and fluorescence measurement experimental details. This material is available free of charge via the Internet at http://pubs.acs.org.

References

(1) Michalet, X.; Pinaud, F. F.; Bentolila, L. A.; Tsay, J. M.; Doose, S.; Li, J. J.; Sundaresan, G.; Wu, A. M.; Gambhir, S. S.; Weiss, S. *Science* **2005**, *307*, 538–544.
(2) (a) Cherukuri, P.; Bachilo, S. M.; Litovsky, S. H.; Weisman, R. B. *J. Am. Chem. Soc.* **2004**, *126*, 15638–15639. (b) Cherukuri, P.; Gannon, C. J.; Leeuw, T. K.; Schmidt, H. K.; Smalley, R. E.; Curley, S. A.; Weisman, R. B. *Proc. Natl. Acad. Sci. U.S.A.* **2006**, *103*, 18882–18886.
(3) Sun, Y. P.; et al. *J. Am. Chem. Soc.* **2006**, *128*, 7756–7757.
(4) Liu, H. P.; Ye, T.; Mao, C. D. *Angew. Chem., Int. Ed.* **2007**, *46*, 6473–6475.
(5) Bourlinos, A. B.; Stassinopoulos, A.; Anglos, D.; Zboril, R.; Georgakilas, V.; Giannelis, E. P. *Chem. Mater.* **2008**, *20*, 4539–4541.
(6) Zhao, Q. L.; Zhang, Z. L.; Huang, B. H.; Peng, J.; Zhang, M.; Pang, D. W. *Chem. Commun.* **2008**, 5116–5118.
(7) Selvi, B. R.; Jagadeesan, D.; Suma, B. S.; Nagashankar, G.; Arif, M.; Balasubramanyam, K.; Eswaramoorthy, M.; Kundu, T. K. *Nano Lett.* **2008**, *8*, 3182–3188.
(8) (a) Huang, H.; Pierstorff, E.; Osawa, E.; Ho, D. *Nano Lett.* **2007**, *7*, 3305–3314. (b) Shenderova, O.; McGuire, G. In *Nanomaterials Handbook*; Gogotsi, Y., Ed.; CRC Press: Boca Raton, FL, 2006; pp 203−238. (c) Mitura, S.; Mitura, K.; Niedzielski, P.; Louda, P.; Danilenko, V. V. *Journal of Achievements in Materials and Manufacturing Engineering* **2006**, *16*, 9–16. (d) Bakowicz-Mitura, K.; Bartosz, G.; Mitura, S. *Surf. Coat. Technol.* **2007**, *201*, 6131–6135. (e) Lam, R.; Chen, M.; Pierstorff, E.; Huang, H.; Osawa, E. J.; Ho, D. *ACS Nano* **2008**, *2*, 2095–2102. (f) Liu, K. K.; Cheng, C. L.; Chang, C. C.; Chao, J. I. *Nanotechnology* **2007**, *18*. (g) Schrand, A. M.; Huang, H. J.; Carlson, C.; Schlager, J. J.; Osawa, E.; Hussain, S. M.; Dai, L. M. *J. Phys. Chem. B* **2007**, *111*, 2–7. (h) Puzyr, A. P.; Baron, A. V.; Purtov, K. V.; Bortnikov, E. V.; Skobelev, N. N.; Mogilnaya, O. A.; Bondar, V. S. *Diamond Relat. Mater.* **2007**, *16*, 2124–2128.
(9) Yu, S. J.; Kang, M. W.; Chang, H. C.; Chen, K. M.; Yu, Y. C. *J. Am. Chem. Soc.* **2005**, *127*, 17604–17605.
(10) Fu, C. C.; Lee, H. Y.; Chen, K.; Lim, T. S.; Wu, H. Y.; Lin, P. K.; Wei, P. K.; Tsao, P. H.; Chang, H. C.; Fann, W. *Proc. Natl. Acad. Sci. U.S.A.* **2007**, *104*, 727–732.
(11) Chen, J.; Hamon, M. A.; Hu, H.; Chen, Y. S.; Rao, A. M.; Eklund, P. C.; Haddon, R. C. *Science* **1998**, *282*, 95–98.
(12) Osswald, S.; Yushin, G.; Mochalin, V.; Kucheyev, S. O.; Gogotsi, Y. *J. Am. Chem. Soc.* **2006**, *128*, 11635–11642.
(13) Mochalin, V.; Osswald, S.; Gogotsi, Y. *Chem. Mater.* **2009**, *21*, 273–279.

JA9004514